ARTICLE

Check for updates

# Traffic restrictions during the 2008 Olympic Games reduced urban heat intensity and extent in Beijing

Bo Yang [1]✉, Hongxing Liu[2]✉, Emily L. Kang [3], Timothy L. Hawthorne[4], Susanna T. Y. Tong[5], Song Shu[6] & Min Xu[7]

Satellite thermal remote sensing has been utilized to examine the urban heat dynamics in relation to the urban traffic restriction policy. During the 2008 Olympic Games in Beijing, the traffic volume was approximately cut off by half through the road space rationing. Based on daily MODIS satellite thermal observations on the surface temperature, statistical models were developed to analyze the contribution of traffic volume reduction to the urban heat intensity and spatial extent. Our analyses show that cutting off half of the traffic volume has led to a marked decrease in the mean surface temperature by 1.5–2.4 °C and shrinkage of the heat extent by 820 km^2 in Beijing. This research suggests that the impact of urban traffic on heat intensity is considerably larger than previously thought, and the management of urban traffic and vehicle fossil fuel use should be included in the future urban heat mitigation plan.

[1] Department of Urban and Regional Planning, San José State University, San José, CA 95192, USA. [2] Department of Geography, University of Alabama, Tuscaloosa, AL 35487, USA. [3] Division of Statistics and Data Science, Department of Mathematical Sciences, University of Cincinnati, Cincinnati, OH 45221, USA. [4] Department of Sociology, University of Central Florida, Orlando, FL 32816, USA. [5] Department of Geography, University of Cincinnati, Cincinnati, OH 45221, USA. [6] Department of Geography and Planning, Appalachian State University, Boone, NC 28608, USA. [7] College of Marine Science, University of South Florida, St Petersburg, FL 33701, USA. ✉email: bo.yang02@sjsu.edu; Hongxing.Liu@ua.edu

rbanization has been taking place at an unprecedented pace around the world in the past decades. In conjunction with the agglomerations of population and economic activities, urban traffic has increased rapidly to meet the needs for mobility and accessibility to different parts of the urban areas. Cities only cover about 1% of the Earth's surface, but they disproportionately consume about 78% of the world's energy and produce more than 60% of all CO_2 emissions[1]. The most apparent expression of the impact of urbanization on the environment is the Urban Heat Island (UHI) effect[2], which refers to the phenomenon where the urban areas have a temperature considerably higher than the surrounding rural areas[3]. High temperatures in urban areas exacerbate thermal discomfort of city dwellers and increase human health risks (e.g., respiratory illnesses, cardiovascular mortality)[4]. The UHI effect greatly boosts energy consumption in cooling, accelerates air pollution in the form of urban smog, surface dioxide and greenhouse gas emissions, and contributes to global warming[1,5]. UHI effect has been recognized as one of the key indicators of environmental change and global climate change[6].

The urban thermal environment is determined by the surface and atmosphere energy balance in urban areas[7,8]. The urbanization process modifies the land surface from natural rural landscape to artificial urban built-up fabric and substantially alters the energy balance and local climate. The proliferation of artificial urban construction materials (e.g. asphalt, concrete, tar and gravel pavements) with low albedo and high heat storage capacity absorbs and accumulates much more of solar radiation[8]. Anthropogenic heat discharge in urban areas[9,10] represents the other major heat component contributing to the formation of UHI. Urban population and industries consume large quantity of fossil fuels for heating and cooling buildings, lighting streets and buildings, manufacturing goods and services, and transporting people and goods. There are two types of anthropogenic heat sources: stationary source from buildings, industries, and public infrastructure, and mobile source from automobiles. Previous studies suggested that the anthropogenic heat has smaller effect than the land surface modification in albedo and vegetation cover and is negligible in commercial and residential areas. Anthropogenic heat discharge in a large city can create a heat island of up to 2–3 °C both during the day and at night[9,11].

Some studies have explored the effect of urban transport and road traffic on the UHI[12–14]. However, most of these studies were qualitative examinations of possible thermal effects of urban traffic in relation to urban road network and traffic density distribution. Little research has been reported on quantitative evaluation of the impacts of urban traffic on the urban thermal environment and heat intensity. The daily operations of urban automobiles (cars, trucks, buses, motorcycles, etc.) generate a large amount of artificial exhaust heat that immediately increases the temperature and emits waste greenhouse gases, which pollute the air and induce a screening effect for the long-term warming[15]. According to US Environmental Protection Agency (EPA), transportation accounts for 28.9% of the total greenhouse emissions, followed by electricity production (27.5%), industry (22.2%), commercial and residential (11.6%), agriculture (9%), and land use (11%)[16]. Nevertheless, the urban traffic effect is difficult to be quantified, since the mobile anthropogenic heat from automobiles is mixed with stationary anthropogenic heat sources from buildings, infrastructure and industries[8].

In this study, we attempt a quantitative assessment on the effect of the anthropogenic heat generated by automobiles on the urban thermal environment, based on the time series Moderate-resolution Imaging Spectroradiometer (MODIS) satellite observations on land surface temperature during a special event, 2008 Olympic Games, with traffic restriction in the Beijing metropolitan area. As the capital of China, Beijing has experienced rapid economic growth and urban expansion since the national economic reform and open-door policy in 1978[17]. The municipality of Beijing (Fig. 1) has an area of 16,411 km^2, and more than 13 million permanent residents and 5 million seasonal workers in 2010[18]. As the major transportation hub of the national highway network, Beijing had 3.3 million registered vehicles in 2008[15,19]. Recorded warming in Beijing since the early 1960s is almost twice as large as the global mean temperature warming trend[20].

Traffic congestion and air pollution were the two major challenges for the execution of the 2008 Olympic Games in Beijing[21]. To ensure good air quality and to alleviate the traffic congestion problem, Beijing municipal government implemented a large-scale short-term traffic restriction policy, namely, the odd-and-even number rule, during the Olympic Games from July 20 to September 20, 2008. During this two-month period, vehicles with even and odd license plate numbers were alternately allowed on road[22,23]. Only the vehicles with even plate numbers can be allowed on the road on one day, and the vehicles with odd plate numbers on the following day. Thus, the odd-and-even number traffic restriction effectively reduced the daily traffic volume by about half during the Olympic Games, compared with the normal traffic volume before and after the Olympic Games. This traffic restriction provided an extraordinary opportunity to observe and examine the impact of traffic volume variation on the urban thermal environment.

Results

We derived urban heat extent and intensity measurements for the Beijing metropolitan area in three summer months (from July 1 to September 30) in 2007 and 2008, by employing daily MODIS satellite thermal observations. The valid urban heat extent and intensity measurements derived from the MODIS data during the Olympic Games between July 20 and September 20 in 2008 are used to form the case group (also known as experimental group) for our statistical analysis, in which the odd-and-even number traffic restriction policy was enforced. The derived urban heat extent and intensity measurements in summer months (July 1–September 30) of 2007 and during the periods from July 1 to 19 (pre-Olympic) and from September 21 to 30 in 2008 are used to form the control group, when no traffic restriction policy was imposed (Table 1). The subdivision of thermal observations and measurements into the case and control groups and the use of traffic restriction dummy variable allow us to successfully isolate and quantify the impact of traffic volume on shaping and regulating the urban thermal environment. Our analysis results show that the half traffic volume reduction led to a shrinkage of the urban heat field (with a surface temperature higher than 35 °C) by about 820 km^2 and also resulted in a marked decrease in the mean surface temperature by 1.5–2.4 °C in Beijing. Our results indicate that the traffic impact on the urban thermal environment may be significantly larger than what the previous studies suggested[9,11,24].

Traffic impact on urban heat extent. We derived the daily surface temperature for the Beijing metropolitan area based on the MODIS satellite thermal images, and then measured the spatial extent of the urban heat field that has a surface temperature higher than a threshold value. The daily spatial extent measurements of the urban heat field (SE$_t$) are then regressed with the net radiation variable and traffic restriction dummy variable to construct a linear regression model for assessing the traffic impact on urban heat extent.

Figure 2a, b show the time series of the urban heat field over the Beijing metropolitan area, respectively, in the morning and
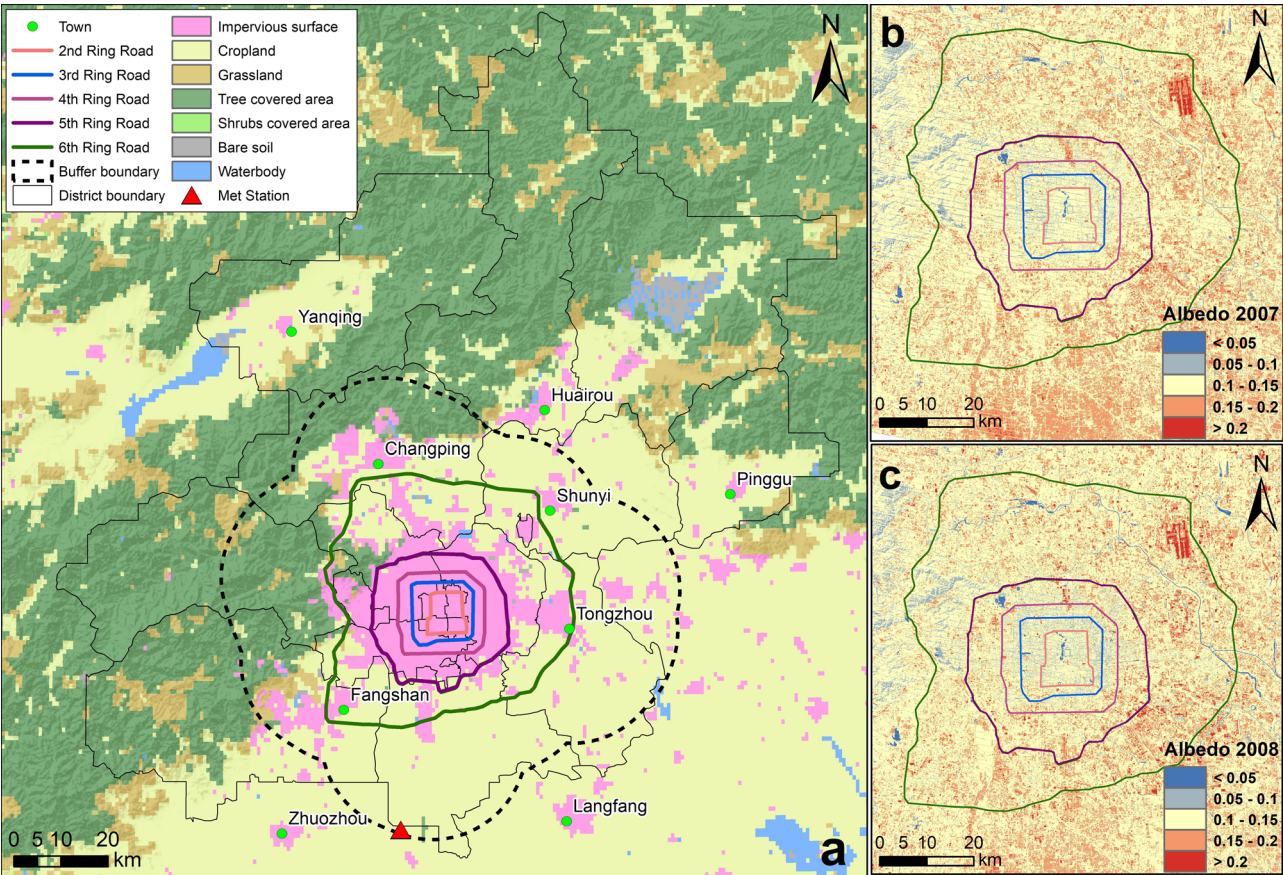
Fig. 1 The case study area in Beijing with land cover types, ring roads, and albedo maps in 2007 and 2008. a Beijing City boundary, ring roads, and land cover types. **b** Albedo map in 2007. **c** Albedo map in 2008.

Table 1 Cloud-free Terra and Aqua MODIS image data for case group and control group.

Daytime	Terra (Morning)		Aqua (Afternoon)	
Time period	07/01–09/30 (2007)	07/01–09/30 (2008)	07/01–09/30 (2007)	07/01–09/30 (2008)
Total images	92	92	92	92
Cloud-free images	17	19	23	18
Images w/ RSR	0	16	0	13

afternoon. The morning time series was derived from Terra MODIS thermal observations, while the afternoon time series from Aqua MODIS observations. Following Meehl et al. [25], we used the 81st percentile of the frequency distribution of observed maximum temperatures as the threshold (T_{thrd}), to define the high-temperature urban heat field, which results in the selection of 35 °C as the threshold value. To evaluate the sensitivity of the threshold, one smaller value (34 °C) and one larger value (36 °C) are also used as additional thresholds for extracting the high-temperature urban heat fields. In Fig. 2a, b, the pixels with a surface temperature below 34 °C are coded in blue color. The pixels with a surface temperature of 34, 35, and 36 °C are, respectively, coded in dark green, light green, and yellow color. The pixels with a surface temperature higher than 36 °C are coded in orange, red and dark red color. The image pixels with a surface temperature larger than the threshold value are combined to calculate the spatial extent of high-temperature urban heat field

for each day. As shown in Fig. 2, the spatial extent of urban heat field change from day to day. The spatial extent of high-temperature urban heat field is the largest on July 3 and 12, 2008, and the smallest on September 25 and 20, 2007.

The spatial extents of high-temperature urban heat field determined by three temperature threshold values of 34, 35, and 36 °C are regressed with the net radiation variable and traffic restriction dummy variable, resulting in three regression equations for the morning observations and three regression equations for the afternoon observations as shown in Table 2. All independent variables are statistically significant in explaining the spatial dynamics of the high-temperature urban heat field. In the morning, the net radiation and traffic restriction explain 57%, 55%, and 54% of the total variation of high-temperature heat field extent defined by surface temperature thresholds of 34, 35, and 36 °C, respectively. The regression modeling results show that the implementation of the traffic restriction policy decreased the spatial extent of high-temperature heat field in the morning by 945.7, 748.8, and 551.8 km^2 for the thresholds of 34, 35, and 36 °C, respectively. Similarly, in the afternoon, both the independent variables are statistically significant, and they are combined to explain about 60% of the spatial extent dynamics of high-temperature urban heat field, as indicated by the value of R^2 (Table 2). The traffic restriction during the Olympic Games reduced the spatial extent of high-temperature urban heat field in the afternoon by 863.7, 905.7, and 908.2 km^2 for thresholds of 34, 35, and 36 °C, respectively. In comparison, the impact of traffic volume reduction on the urban heat extent is stronger in the afternoon than in the morning. The average areal shrinkage of the heat spatial extent due to the traffic restriction is about 820 km^2.
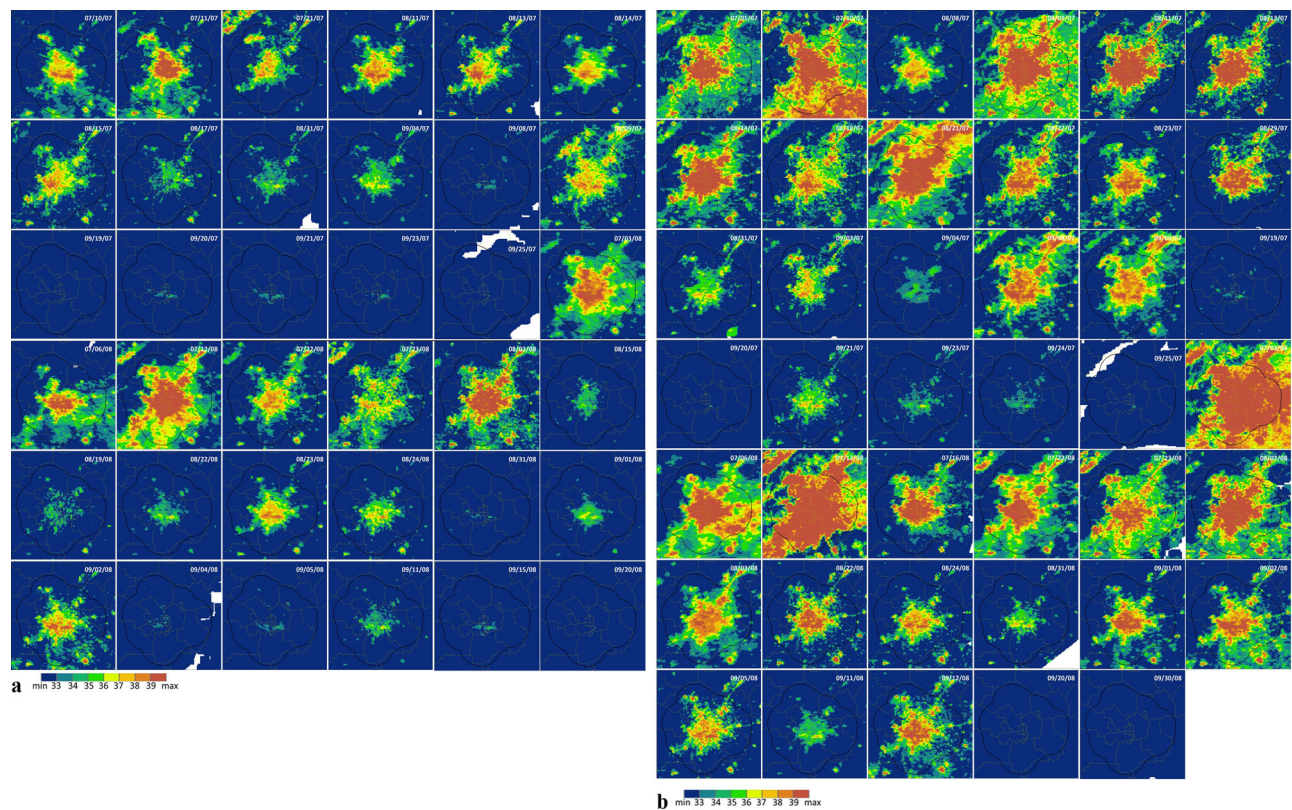
Fig. 2 Morning and afternoon urban land surface temperatures in Beijing in 2007 and 2008. Land surface temperature (°C) time series for: **a** morning derived from Terra MODIS, and **b** afternoon derived from Aqua MODIS observations.

Table 2 Statistical model of urban heat spatial extent.

Daytime	T_{thrd} (°C)	Fitted regression model	R^2	p-value
Morning(10:30 a.m.)	34	$SE_t = 1.75 \times R_n - 945.7 \times RSR_t - 3503.8$	0.57	R_n: 0.0000, RSR_t: 0.0072
	35	$SE_t = 1.33 \times R_n - 748.8 \times RSR_t - 2748.8$	0.55	R_n: 0.0000, RSR_t: 0.0077
	36	$SE_t = 0.99 \times R_n - 551.8 \times RSR_t - 2118.0$	0.54	R_n: 0.0000, RSR_t: 0.0088
Afternoon (1:30 p.m.)	34	$SE_t = 2.57 \times R_n - 863.7 \times RSR_t - 703.1$	0.58	R_n: 0.0000, RSR_t: 0.0493
	35	$SE_t = 2.31 \times R_n - 905.7 \times RSR_t - 4453.9$	0.59	R_n: 0.0000, RSR_t: 0.0218
	36	$SE_t = 2.03 \times R_n - 908.2 \times RSR_t - 4094.5$	0.60	R_n: 0.0000, RSR_t: 0.0082

Traffic impact on urban heat intensity. We use the mean surface temperature to represent the urban heat intensity. Based on the surface temperature measurements derived from MODIS satellite thermal observations, we calculated the daily mean surface temperature for each of six circular zones in the Beijing metropolitan area. The mean surface temperature for each zone as the response/dependent variable is regressed on the net radiation variable and traffic restriction dummy variable to construct statistical models, which are used for assessing the impact of the traffic restriction and associated traffic volume reduction on the urban heat intensity.

The Beijing metropolitan area has multiple ring roads around the central business district[26], which divide the metropolitan area into several concentric ring zones (Fig. 1). We denote the inner urban area inside 2nd ring road by Zone 1, the urban area between 2nd and 3rd ring roads by Zone 2, the urban area between 3rd and 4th ring roads by Zone 3, the urban area between 4th and 5th ring roads as Zone 4, and the urban area between 5th and 6th ring roads by Zone 5. Zone 6 denotes the 20 km outward buffer zone from 6th ring road, the outmost ring road in the Beijing metropolitan area. The traffic restriction was only applied to the Beijing metropolitan area inside the 5th ring road during the 2008

Olympic Games. However, the traffic restriction inside the 5th ring road has indirectly reduced the traffic volume in Zone 6 (outside the 5th ring road) due to smaller traffic flow from the inner city[19,22,27].

By using Terra MODIS satellite observations, we constructed six statistical models to express the relationship of the urban heat intensity of each zone in the morning with the net radiation and the traffic restriction policy (Table 3). Similarly, six statistical models were also constructed for assessing urban heat intensity in the afternoon by using Aqua MODIS satellite observations (Table 3). As shown in Table 3, the impacts of net radiation and traffic restriction on urban heat intensity are statistically significant. As indicated by the value of R^2, those independent variables are combined to explain over 50% of the variations of the heat intensity in the morning for all urban zones except for Zone 6. Large agriculture and vegetated lands are distributed in Zone 6, which has a relatively low impervious surface coverage (Fig. 1). This zone appears less sensitive to the traffic volume variation in the morning. The reduction in the mean surface temperature associated with the traffic restriction during the 2008 Olympic games was 1.69, 1.65, 1.63, 1.59, and 1.56 °C from Zone 1 to Zone 5 (Table 3). The regression modeling results for the afternoon observations show that the impacts of the traffic

Table 3 Statistical model of urban heat intensity.

Daytime	Zone	Fitted regression model	R^2	p-value
Morning (10:30 a.m.)	Zone 1	$HI_t = 0.0043 \times R_n - 1.69 \times RSR_t + 23.22$	0.53	R_n: 0.0000, RSR_t: 0.0556
	Zone 2	$HI_t = 0.0044 \times R_n - 1.65 \times RSR_t + 22.71$	0.56	R_n: 0.0000, RSR_t: 0.0486
	Zone 3	$HI_t = 0.0043 \times R_n - 1.63 \times RSR_t + 23.22$	0.55	R_n: 0.0000, RSR_t: 0.0478
	Zone 4	$HI_t = 0.0039 \times R_n - 1.59 \times RSR_t + 23.46$	0.53	R_n: 0.0000, RSR_t: 0.0438
	Zone 5	$HI_t = 0.0033 \times R_n - 1.56 \times RSR_t + 23.20$	0.50	R_n: 0.0000, RSR_t: 0.0385
	Zone 6	$HI_t = 0.0026 \times R_n - 1.60 \times RSR_t + 25.61$	0.40	R_n: 0.0000, RSR_t: 0.0200
Afternoon (1:30 pm)	Zone 1	$HI_t = 0.0064 \times R_n - 2.44 \times RSR_t + 20.24$	0.61	R_n: 0.0000, RSR_t: 0.0197
	Zone 2	$HI_t = 0.0063 \times R_n - 2.37 \times RSR_t + 20.21$	0.63	R_n: 0.0000, RSR_t: 0.0177
	Zone 3	$HI_t = 0.0061 \times R_n - 2.27 \times RSR_t + 20.77$	0.63	R_n: 0.0000, RSR_t: 0.0199
	Zone 4	$HI_t = 0.0055 \times R_n - 1.83 \times RSR_t + 21.49$	0.62	R_n: 0.0000, RSR_t: 0.0387
	Zone 5	$HI_t = 0.0047 \times R_n - 1.71 \times RSR_t + 21.38$	0.60	R_n: 0.0000, RSR_t: 0.0321
	Zone 6	$HI_t = 0.0041 \times R_n - 1.50 \times RSR_t + 20.62$	0.56	R_n: 0.0000, RSR_t: 0.0409

restriction on the heat intensity for all concentric urban zones are statistically significant. The reduction in mean surface temperature induced by the traffic restriction during the Olympic Games is 2.44, 2.37, 2.27, 1.83, 1.71, and 1.50 °C from Zone 1 to Zone 6 in the afternoon (Table 3). It appears that the reduction level in the heat intensity by the traffic restriction gradually decreases outward from the urban center to the urban fringe zones in both morning and afternoon. In comparison, the heat intensity reduction effect of the traffic restriction in the afternoon is considerably stronger than in the morning.

Urban heat spatial extent and intensity at nighttime. We also derived the time series urban surface temperature maps at nighttime by employing Terra MODIS overpasses at 10:30 p.m. and Aqua MODIS overpasses at 1:30 a.m. local time. Figure 3 shows the nighttime surface temperature evolution in the Beijing metropolitan area before, during and after the Olympic Games, which derived from Aqua MODIS satellite thermal observations at local time of 1:30 a.m. Note that the surface temperature color scheme for nighttime in Fig. 3 is different from the daytime in Fig. 2. Apparently, urban surface temperatures at nighttime are significantly lower than at daytime. The thermal spatial structure remains a concentric pattern and the surface temperature decreases from the urban center to the rural periphery.

By using the threshold value of 23 °C, we defined the nighttime heat spatial extent. The statistical analysis results for nighttime heat spatial extent at 10:30 p.m. (based on Terra MODIS observation) and 1:30 a.m. (based on Aqua MODIS observations) are shown in Table 4. As indicated by the values of R^2, the models only explain <20% of nighttime (10:30 p.m. or 1:30 a.m.) heat spatial extent variation. The impact of net radiation variable (R_n) is statistically significant, as indicated by its p-value ≤ 0.05. But, the p-value of the traffic restriction variable (RSR_t) is away higher than 0.05, which indicates the failure to reject the null hypothesis and no statistical relationship between traffic restriction policy and nighttime heat spatial extent.

By using Terra and Aqua MODIS nighttime overpasses, we derived the mean nighttime surface temperatures for different urban zones. The statistical models for nighttime urban heat intensity at 10:30 p.m. (based on Terra MODIS observation) and 1:30 a.m. (based on Aqua MODIS observations) are shown in Table 5. As indicated by the values of R^2, statistical models only explain less than 45% of nighttime (10: 30 p.m. or 1:30 a.m.) heat intensity variations for all urban zones. Again, the impact of net radiation variable (R_n) on the urban heat intensity is statistically significant, as indicated by its p-value ≤ 0.05. However, the impact of the traffic restriction variable (RSR_t) on nighttime heat spatial extent is not statistically significant, as indicated by its very large p-values.

Discussion

Although anthropogenic heat discharge has been identified as an important factor contributing to the formation of UHI effect[18,28], little has been known about the impacts of different anthropogenic sources on the urban thermal environment[9,24]. Since the mobile anthropogenic heat from automobiles is mixed with stationary anthropogenic heat from buildings, infrastructure and industries[8], it has long been difficult to separate and quantify the impact of mobile anthropogenic source from stationary anthropogenic. Some studies have qualitatively examined the influences of urban road network and traffic density on the urban thermal environment[12,13,29], but the magnitude of the urban traffic heat effect has not been quantified in previous studies.

By taking advantage of satellite thermal observations and drastic urban traffic volume variation during the 2008 Olympic Games, we were able to statistically assess the effect of the anthropogenic heat emission generated by automobiles of urban transportation system on the urban thermal environment. Our study period consists of two adjacent summer seasons in 2007 and 2008, and the odd-and-even number traffic restriction policy was imposed from July 20 to September 20, 2008 to support the Olympic Games activities, which dramatically reduced the urban traffic volume. In our research design, we have constrained our satellite observations of the case group (July 20–September 20, 2008) and control group (July 1–September 30, 2007; July 1–19, September 21–30, 2009) to a relatively short time period of the same season to minimize possible variations in land cover and stationary anthropogenic source. By using Landsat-7 multispectral images in summers of 2007 and 2008, we verified the land cover changes are minimal, and the slight albedo variation between 2007 and 2008 summers has been incorporated in the calculation of the explanatory variable of net radiation. The stationary anthropogenic heat source from buildings and factories was relatively stable and very similar in the case period and control period, which was reflected by similar annual electricity consumption between 2007 and 2008[30] and similar monthly electricity production in July, August, and September of 2007 and 2008 in Beijing[31]. Based on the urban surface energy balance equation, we determined that the daily land surface temperature variation in our study period was primarily influenced by the variations of the solar radiation intensity, surface albedo and traffic volume (mobile anthropogenic heat), which provides the physical basis for our multiple regression models. The variations of solar radiation intensity and surface albedo are reflected by the net radiation explanatory variable, which virtually accounts for the effect of the climate/weather differences in 2007 and 2008. By innovatively introducing a dummy variable for the traffic restriction policy in the regression models, we are able to statistically quantify the impacts of urban traffic volume variation
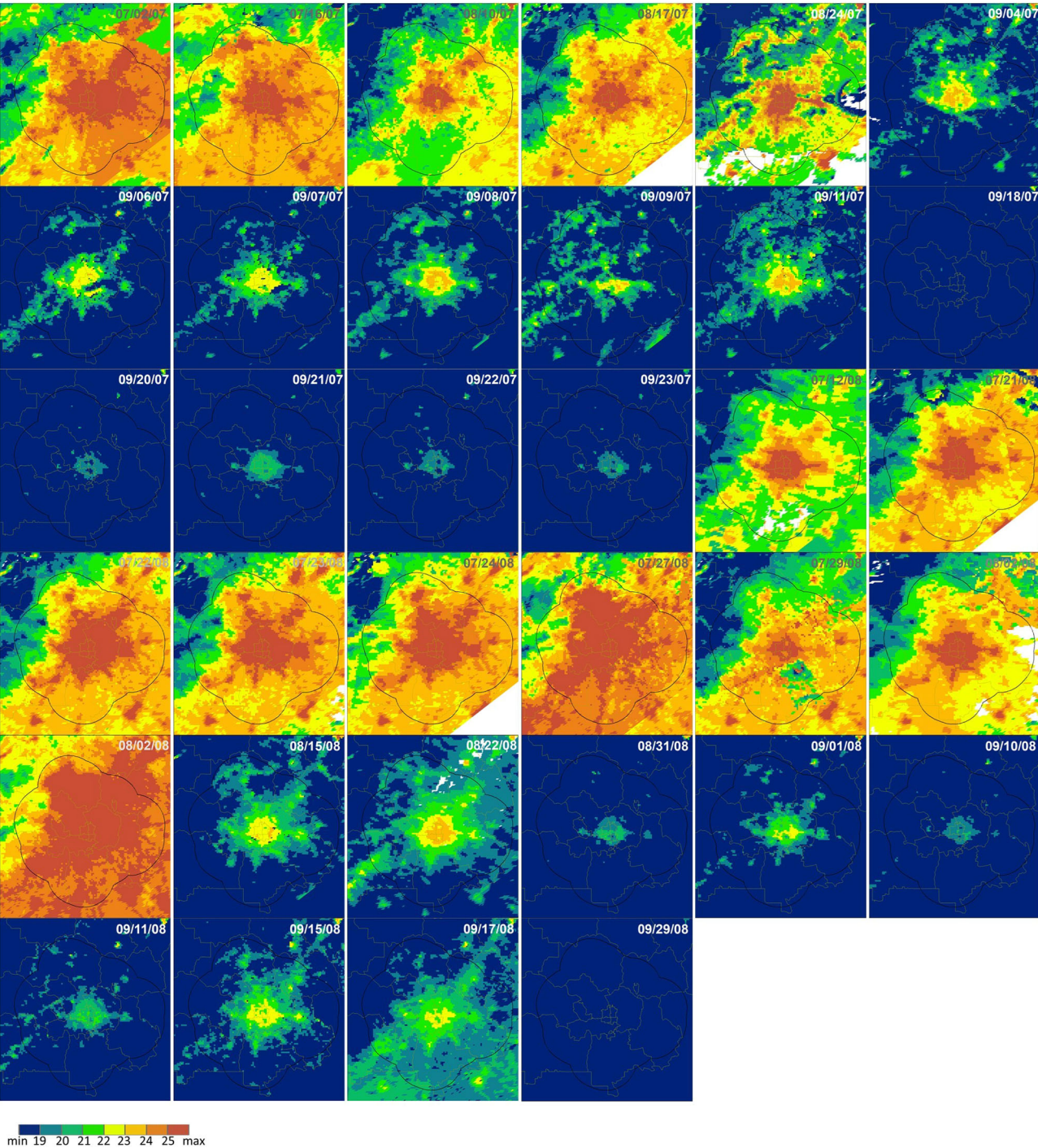
Fig. 3 Night time urban land surface temperatures in Beijing in 2007 and 2008. Land surface temperature (°C) time series during night time (01:30 a.m.) derived from Aqua MODIS observations.

Table 4 Statistical model of urban heat spatial extent at nighttime.

Nighttime	T_{thrd} (°C)	Fitted regression model	R^2	p-value
Terra (10:30 p.m.)	23	$SE_t = 2.88 \times R_n - 608.1 \times RSR_t - 1040.9$	0.19	R_n: 0.0011, RSR_t: 0.2869
Aqua (1:30 a.m.)	23	$SE_t = 0.09 \times R_n - 357.8 \times RSR_t - 565.2$	0.17	R_n: 0.0158, RSR_t: 0.4069

induced by the traffic restriction policy on the spatial extent and intensity of urban heat field.

Our analysis results show that the traffic restriction and associate traffic volume variation is statistically significant in influencing the heat intensity for all urban zones. The traffic restriction during the Olympic Games effectively reduced the mean land surface temperature by 1.5–2.4 °C, depending on the urban zone. During the Olympic Games, besides the odd-and-

Table 5 Statistical model of urban heat intensity at nighttime.

Nighttime	Zone	Fitted regression model	R^2	p-value
Terra (10:30 p.m.)	Zone 1	$HI_t = 0.0062 \times R_n - 0.17 \times RSR_t + 14.72$	0.37	R_n: 0.0000, RSR_t: 0.8259
	Zone 2	$HI_t = 0.0067 \times R_n - 0.30 \times RSR_t + 15.55$	0.41	R_n: 0.0000, RSR_t: 0.6877
	Zone 3	$HI_t = 0.0069 \times R_n - 0.31 \times RSR_t + 16.22$	0.43	R_n: 0.0000, RSR_t: 0.6738
	Zone 4	$HI_t = 0.0071 \times R_n - 0.46 \times RSR_t + 16.37$	0.45	R_n: 0.0000, RSR_t: 0.5242
	Zone 5	$HI_t = 0.0071 \times R_n - 0.34 \times RSR_t + 16.29$	0.43	R_n: 0.0000, RSR_t: 0.6502
Aqua (1:30 a.m.)	Zone 1	$HI_t = 0.0003 \times R_n - 0.12 \times RSR_t + 16.52$	0.33	R_n: 0.0006, RSR_t: 0.9106
	Zone 2	$HI_t = 0.0003 \times R_n - 0.12 \times RSR_t + 16.53$	0.33	R_n: 0.0006, RSR_t: 0.9094
	Zone 3	$HI_t = 0.0003 \times R_n - 0.03 \times RSR_t + 16.03$	0.33	R_n: 0.0007, RSR_t: 0.9710
	Zone 4	$HI_t = 0.0003 \times R_n - 0.06 \times RSR_t + 16.17$	0.31	R_n: 0.0011, RSR_t: 0.9559
	Zone 5	$HI_t = 0.0003 \times R_n - 0.14 \times RSR_t + 14.29$	0.28	R_n: 0.0026, RSR_t: 0.8999

even number rule, 70% of the vehicles owned by the governments, state enterprises and public institutions were suspended for the use, the high-emission vehicles with a yellow label were banned from the roads, trucks were not allowed inside the 6th Ring Road during the daytime. Essential service vehicles (police cars, fire trucks, ambulances, postal vehicles, taxis), and public transit vehicles (buses, trolleys, and subway) were exempt to the traffic restriction[22]. The traffic restriction during the 2008 Olympic Games in Beijing actually cut down nearly 1.95 million vehicles on road[15,19], which was 54% of vehicles registered in Beijing[19,22]. Assuming the linear relationship, the average heat effect of 1 million vehicles would be 1–1.64 °C. Given the total vehicle number of 3.3 million in Beijing in 2008[15,19], the total heat effect of urban traffic would be 3.3–5.4 °C.

Like many other cities in the world, Beijing's traffic flow exhibits a double-peak pattern[32]. Its morning traffic peak occurs during 7:00–8:30 a.m. and the evening traffic peak occurs during 5:00–6:30 p.m.[26,33]. The Terra MODIS satellite overpasses Beijing at 10:30 a.m., about 2 h after the morning traffic rush hour. The Aqua MODIS satellite overpasses Beijing at 1:30 pm, about four hours earlier than the afternoon traffic rush hour. Therefore, the actual magnitude of the traffic heat effect in rush hours could be even larger than our estimate based on Terra and Aqua MODIS satellite observations.

Previous studies suggest that the whole anthropogenic heat from buildings and vehicles may contribute 2–3 °C temperature increase both during the day and at night[9,11] and that the anthropogenic heat has a smaller impact than albedo and vegetation cover, thus negligible in commercial and residential areas[9,24]. In comparison, the heat effect of the mobile anthropogenic source alone estimated from our study based on actual meteorological and thermal remote sensing data is remarkably larger than the combined effect of both stationary and mobile anthropogenic sources reported in the previous studies. Therefore, the actual contribution of the anthropogenic heat sources, particularly the urban traffic, to the urban thermal environment may be considerably larger than previously thought. We acknowledge that such a comparison with previous studies is crude and preliminary, and more rigorous investigation in this aspect is needed in future study.

Our analysis results also reveal that the heat effect of the urban traffic is not homogeneous in space and time. The spatial and temporal heterogeneity of the traffic heat effect is probably caused by the spatial variation in population density and urban functions, and temporal patterns of human activities. The Beijing metropolitan area has a concentric spatial structure. Zone 1 includes Dongcheng and Xicheng districts, which are the central business district and old downtown[26], Zone 2 and Zone 3 include Haidian, Chaoyang, Fengtai, and Shijingshan districts, where commercial, high tech industries, educational institutions are concentrated. Zone 4 and Zone 5 are new urban development

districts with some modern manufacturing, and Zone 6 contains agricultural and ecological conservation lands. We found out that the mitigation effect of the traffic volume reduction on the urban heat intensity decreases outward from the urban center to the urban fringe both in the morning and afternoon. The heat mitigation effect of the traffic restriction during the Olympic Games appears more apparent and stronger in the afternoon than in the morning for all urban zones. This differential effect of traffic volume variation in space and time tends to change the spatial structure of the urban thermal environment.

Our analysis indicates that the influence of urban traffic on the spatial extent of the high-temperature urban field is statistically significant. In the Beijing metropolitan area, the traffic restriction and associated traffic volume reduction of 1.95 million vehicles[15,22] during the Olympic Games effectively reduced the spatial extent of the high-temperature urban heat field. With the threshold of 35 °C to define the spatial extent of high-temperature heat field, our statistical modeling results show that the traffic restriction and associated traffic volume reduction effectively reduced the urban heat extent by 748.8 km² in the morning and by 905.7 km² in the afternoon, which accounts for 12.4–15.0% of our case study area-the Beijing metropolitan area. On the assumption of the linear relationship, the traffic decrease by 1 million vehicles may lead to the shrinkage of high-temperature urban field by 394 km² in the morning and 477 km² in the afternoon on average. To examine the sensitivity of our analysis results to the selection of temperature threshold, we also tested a lower threshold value (34 °C) and a higher threshold value (36 °C) to define the spatial extent of high-temperature urban heat field, and both threshold values resulted in similar and consistent estimate results. This indicates that our findings are reliable and robust, insensitive to the selection of the threshold value.

The traffic restriction based upon the last digits of the license number during a certain period, also known as road space rationing or alternate-day travel scheme, has been practiced in many cities during major international events for cleaning the air and relieving traffic congestion, such as São Paulo (1997), México City for what (1989), Metro Manila (1995), Paris (2016)[34], Beijing for the Olympic Games (2008) and for the Asia-Pacific Economic Cooperation (APEC) forum (2014). During the 2008 Olympic Games in Beijing, the traffic restriction was imposed and enforced for 62 days[34]. Such a long period of traffic restriction allows us to select a sufficient number of cloud-free MODIS thermal images in the case group to support a reliable and robust statistical analysis of the traffic volume effect on the urban heat dynamics. It should be noted that the primary objectives of the traffic restriction during the 2008 Olympic Games are to mitigate traffic congestion and to reduce ambient air pollution[26,35]. Our study suggests that the traffic restriction has additional benefit in the effective reduction of urban heat intensity and extent.

Most previous UHI studies emphasized the roles of the increasing urban construction materials and impervious surface, the decreasing vegetation cover and moisture content, and the canyon-like morphology of urban streets in the formation of UHI effect[2,36]. The impact of anthropogenic sources was considerably underestimated or ignored. Consequently, the recommended adaption options and heat mitigation strategies in urban planning and design mainly include high-albedo green and cool roofs and pavements[24,37,38], landscaping with street trees, lawns and ponds[10], urban parks, and urban ventilation corridors[39] to offset the future greenhouse warming. Our study suggests that the heat effect of the anthropogenic sources, particularly the urban traffic, plays an important role in shaping urban thermal environment. The vehicles burn a large quantity of fossil fuels in urban areas to emit artificial exhaust heat and waste greenhouse gases to the urban environment[40], hence causing air pollution and enhancing the urban heat effect (IPCC, 2007). The quantity of waste heat and greenhouse gases from urban traffic not only depends on the number of vehicles, but also on the vehicle model, running speed, and fuel type[12]. The future urban adaptation measures for heat mitigation should also include the control and management of urban traffic and vehicle fossil fuel use. The measurements to ameliorate the urban heat and pollution problems of urban traffic may include the control of vehicle number and density, improvements in running speed, reduction of heat storage volume, increase in vehicle engine efficiency, and improvement of fuel quality.

Our statistical analysis results indicate that the net radiation (solar radiation and albedo) and traffic volume statistically account for about 50–60% of the total observed daily variations of the urban heat intensity and the spatial extent of high-temperature urban heat field in our study period. There are 40–50% variations unexplained, which may come from other factors or measurement errors. For instance, about 40 factories were shut down in Beijing and Tianjin during the Olympic Games to improve air quality[41]. Although those closed factories were far away from the Beijing metropolitan area (>100 km to urban center), they may have the indirect urban heat effect through the screening effect of their reduced greenhouse gases. Further research efforts should be made to identify additional possible factors and variables that influence urban heat dynamics in the future.

It should be emphasized that although traffic restriction policy during the Olympic Games substantially reduced high-temperature urban heat field and decreased the mean surface temperature for all urban zones, its impacts on the nighttime urban heat spatial extent and intensity are minimal and statistically insignificant. It should be noted that the influences of the net radiation are statistically significant for both daytime and nighttime urban thermal environment, even though its influence is stronger at daytime than at nighttime. This indicates that the differential heating effect of solar radiation may last from the daytime to nighttime to a certain extent. Also, it must be recognized that the traffic flow volume reduction associated with the traffic restriction policy during the Olympic Games mainly occurred at daytime between 7:00 a.m. and 9:00 p.m., and the traffic volume at nighttime from 9:00 p.m. to 7:00 a.m. during the Olympic Games was almost the same as in pre-Olympic and post-Olympic periods[19,26,27]. Particularly at Aqua MODIS satellite nighttime overpass time of 1:30 a.m., the urban traffic volume kept a similar small value, no matter whether the traffic restriction policy was enforced or not. Since the traffic restriction policy did not induce the associated traffic volume changes at nighttime, therefore its impact on the nighttime urban thermal environment is negligible, as suggested by our statistical analysis results.

Methods

Satellite observations and in situ datasets. In this research, we employed daily Terra and Aqua MODIS satellite thermal images to derive the surface temperature at a spatial resolution of 1000 m for the Beijing metropolitan area, during the Olympic Games with traffic restrictions against the pre- and post-Olympic observations without the traffic restriction. Landsat-7 ETM+ multispectral image data are used to estimate the albedo and assess possible land cover changes. In situ data from a local meteoritical station are used to represent the solar radiation and weather condition. We used NASA MODIS LST Version 6 (v6) products from both Terra and Aqua satellites. Terra MODIS satellite overpasses Beijing at 10:30 a.m. local time, and its daily thermal images form the time series for the morning. Aqua MODIS satellite overpasses at 1:30 p.m. local time in the afternoon, and its daily thermal images form the other time series for the afternoon. These two separate time series allow us to investigate the urban thermal environment temporal variation of urban heat environment between the morning and afternoon within a day.

We screened all MODIS images acquired from July 1 to September 30 in 2007 and 2008, and selected 77 images for this research (Table 1). Those images with more than 10% cloud coverage were excluded. Since the wind chill effect substantially influences sensible heat and ground heat through convection[42,43], those images acquired on high-wind days (>5 m/s) were also ruled out to ensure model accuracy. Among 36 cloud-free Terra MODIS images, 16 of them were acquired during the Olympic Games with traffic restriction, which constitute the traffic restriction case group in the morning. The remaining 20 cloud-free Terra MODIS images, including 3 images acquired in 2008 and 17 images acquired in 2007 without traffic restriction, constitute the control group in the morning. Similarly, we used 13 cloud-free Aqua MODIS images acquired with the traffic restriction to form the case group in the afternoon, and the remaining 28 cloud-free MODIS images acquired without the traffic restriction to form the control group in the afternoon. It should be noted that the control groups include the summer images from both 2007 and 2008 to address the possible bias between different years.

Two cloud-free Landsat-7 ETM+ multispectral images acquired on September 9 in 2007 and September 11 in 2008 are used to estimate the overall surface albedo in the summers of 2007 and 2008. The surface albedo is the wavelength-integrated reflectivity of surface materials. Typically, urban albedos are in the range of 0.1–0.2[16]. Figure 1b, c show the derived albedo maps in 2007 and 2008. The average albedo for Beijing metropolitan area slightly decreased from 0.145 in 2007 to 0.136 in 2008. The albedo difference has been incorporated to estimate the net radiation variation.

A meteorological station of China Land Data Assimilation System (CLDAS), located at latitude of 39.48°N and longitude of 116.28°E in Beijing (Fig. 1a), recorded the wind speed, total incoming solar radiation, net radiation, and instant radiation (in the unit of Mega Joules per square meter). Solar radiation observations at this station are used to represent and model the temporal variation of net radiation in the statistical models, while the daily wind speed is used to screen and select MODIS thermal images.

Statistical models. Based on the near-surface energy balance model that considers net radiation, anthropogenic heat, the sensible, latent, ground heat fluxes and surface albedo factors[11,44], we developed two sets of statistical models to quantify the effect of traffic restriction and associated traffic volume on the spatial extent and intensity of the urban heat effect. The response variable of the first set of statistical models is the urban heat extent (SE_t) represented by the total urban area with a surface temperature higher than a specified threshold value, while the response variable of the second set of statistical models is the urban heat intensity (HI_t) represented by the mean surface temperature of an urban zone. Both sets of statistical models have the same explanatory (predictor) variables: net radiation variable (R_n) and traffic restriction variable (RSR_t). The net radiation variable (R_n) represents the natural heat source due to variations of incoming solar radiation and the surface albedo, while traffic restriction variable (RSR_t) indicates the variation of mobile anthropogenic heat discharge due to the traffic restriction.

The land surface temperature varies in response to the surface energy balance and is highly correlated with the near-surface air temperature[45]. Surface moisture, thermal admittance and surface emissivity, the radiative input at the surface from the sun and atmosphere, and the interaction between the near-surface atmosphere and the surface all influence the land surface temperature[46,47]. The surface energy balance terms in urban areas are different from the rural areas. In addition to solar radiation input (natural source), the anthropogenic heat discharge (human source) also plays an important role in the urban energy budget. The general form of the surface energy balance in urban areas can be expressed by the following equation[9]:

$$R_n + Q_f = H + \lambda E + G \tag{1}$$

where R_n is net radiation and Q_f is the total anthropogenic heat discharge. On the right side of equation, H, λE, and G are the sensible, latent, and ground heat fluxes, respectively. The sensible energy H heats the lower layers of air through the conductive heat flux from the Earth's surface to the atmosphere. The ground heat G is the storage of energy in land to warm the near-surface soil layers. The latent heat λE is absorbed by the evapotranspiration process, namely the transpiration of vegetation and the evaporation of land surface moisture.

The net radiation (R_n) is the sum of the absorbed incoming short-wave solar and long-wave radiations emitted from the atmosphere. It can be expressed by Eq. (2) below:

$$R_n = (1 - \mu) * I + L \qquad (2)$$

where L is the net long-wave radiation from the atmosphere and the land surface, I is incoming short-wave solar radiation, μ is the surface albedo indicating the ability of the surface material to reflect the incident solar energy back to space.

The combination of Eqs. (1) and (2) results in a modified urban energy balance equation:

$$H + G = (1 - \mu) * I + Q_f + L - \lambda E \qquad (3)$$

The two terms on the left side of Eq. (3), the sensible heat (H) and ground heat (G) control the land surface temperature and near-surface air temperature, which reflect the state of the urban thermal environment. Terms on the right side of Eq. (3) are the factors (variables) influencing the surface and near-surface air temperature. Actually, Eq. (3) explains the roles of key urban land surface properties (the surface albedo, vegetation transpiration, land surface moisture evaporation) and anthropogenic (man-made) heating in forming and shaping the urban thermal environment[9]. In an urbanized area, the decreased vegetation coverage and land moisture source for the evapotranspiration process result in the much lower latent heat flux (λE) to dissipate the absorbed solar heat (R_n) and anthropogenic heat (Q_f). Artificial urban surface materials (e.g. asphalt, concrete, tar and gravel pavements) have a low albedo (μ), and hence absorb and accumulate much more of solar radiations (R_n)[8]. Due to the large concentration of population and economic activities in the urban area, the anthropogenic heat discharge Q_f from residential buildings, factories and transportation make a substantial input source to the urban energy balance, in addition to the natural solar source.

We use the urban surface energy balance in Eq. (3) as the physical basis to determine the response (dependent) variables and explanatory (independent) variables of our statistical models. The high-temperature urban heat field extent and urban heat intensity (mean surface temperature) reflect the combined effect of the sensible heat (H) and ground heat (G), and they are used as the response variables for urban thermal environment. Surface albedo μ, and the radiation R_n are treated as two explanatory variables. Although the vegetation coverage has largely reduced in the Beijing metropolitan area in the past decades, there was no much change in vegetation coverage and impervious surface during our study period 2007–2008. Therefore, the latent heat latent heat flux (λE) is treated as constant for our study period. The stationary anthropogenic heat source (heat discharge from the residential buildings, factories) had a minimal change during 2007–2008 and hence is treated as a constant. The mobile anthropogenic heat from automobiles had a strong variation due to the traffic restriction during the Olympic Games. Therefore, the traffic volume associated with the traffic restriction is treated as an explanatory variable for representing the variation of anthropogenic head discharge (Q_f). Based on the above physical interpretation of the urban surface energy balance equation, the response variables of the high-temperature urban heat field extent and urban heat intensity are modeled as a function of the surface albedo, radiation, and traffic volume in our study time period from June 1, 2007 to September 30, 2008.

The first multiple regression model represents the high-temperature urban heat spatial extent (SE_t), as the linear function of net radiation and the traffic variables as below:

$$SE_t = a_0 + a_1 R_n + a_2 RSR_t + e_t \qquad (4)$$

where SE_t is the high-temperature urban heat extent defined with a temperature threshold at time t. RSR_t is the traffic variable at time t. a_0, a_1 and a_2 are regression coefficients to be estimated, e_t is an error term. The coefficient a_1 represents the impact of net radiation on the spatial extent of high-temperature urban heat field, while the coefficient a_2 of the dummy variable RSR_t represents the impact of the traffic volume variation on the high-temperature heat extent induced by the RSR traffic restriction.

The second multiple regression model represents the urban heat intensity (HI_t) as the linear function of net radiation and the traffic variables:

$$HI_t = b_0 + b_1 R_n + b_2 RSR_t + e_t \qquad (5)$$

where HI_t is the urban heat intensity expressed by the mean surface temperature at time t, b_0, b_1 and b_2 are coefficients to be estimated, e_t is an error term at time t. The coefficient b_1 represents the impact of net radiation on the heat intensity, while the coefficient b_2 represents the impact of the traffic volume variation on the heat intensity. The second multiple regression model was constructed for each of six concentric urban zones in the Beijing metropolitan area.

It should be noted that a qualitative dummy variable (RSR_t) was used in the above multiple regression models to indicate the traffic volume variation. The dummy explanatory variable, also known as an indicator variable[48], allows us to represent the traffic restriction in a standard quantitative regression model, without imposing unrealistic measurement assumptions on the categorical variable. The traffic restriction dummy variable (RSR_t) is set to 1, when the traffic restriction was imposed during the Olympic Games, namely for the MODIS images in the case group acquired during the Olympic Games. The traffic restriction dummy variable (RSR_t) is set to 0, when the traffic restriction was not imposed before or after the

Olympic Games, namely for the MODIS images in the control group acquired before or after Olympic Games. The regression analysis with the dummy variable is able to inform if the impact of the traffic restriction is statistically significant and what is the magnitude of the impact of the traffic restriction on the spatial extent and the intensity of urban heat field. Since the odd-and-even number traffic restriction policy approximately cut off the regular traffic volume by half, the impact magnitudes of the traffic restriction determined through the regression analysis with the dummy variable virtually indicate the magnitude of the impacts of cutting off about half of the regular traffic volume on the extent and intensity of urban heat filed.

In the modeling, the daily net radiation (R_n) was calculated using Eq. (2), based on the observations from the meteorological station on incoming short-wave solar radiation (I), the net long-wave radiation (L), and the surface albedo (μ). A narrowband to broadband conversion algorithm is used to estimate the surface albedo (μ) with the input of Top of Atmosphere (TOA) reflectance of Landsat-7 ETM+ non-thermal bands (1, 3, 4, 5, and 7)[49]. Daily surface temperature from Terra and Aqua MODIS thermal image data was used to extract the urban heat extent (SE_t) and intensity (HI_t).

Data availability

References

1. Estrada, F., Botzen, W. J. W. & Tol, R. S. J. A global economic assessment of city policies to reduce climate change impacts. *Nat. Clim. Chang.* **7**, 403–406 (2017).
2. Swain, D. et al. Impact of rapid urbanization on the city of Bhubaneswar, India. *Proc. Natl Acad. Sci. India Sect. A - Phys. Sci.* **87**, 845–853 (2017).
3. Oke, T. R. The distinction between canopy and boundary-layer urban heat Islands. *Atmosphere (Basel)* **14**, 268–277 (1976).
4. Patz, J. A., Campbell-Lendrum, D., Holloway, T. & Foley, J. A. Impact of regional climate change on human health. *Nature* **438**, 310–317 (2005).
5. Epstein, S. A. et al. Air-quality implications of widespread adoption of cool roofs on ozone and particulate matter in southern California. *Proc. Natl. Acad. Sci.* **114**, 8991–8996 (2017).
6. Zhao, L., Lee, X., Smith, R. B. & Oleson, K. Strong contributions of local background climate to urban heat islands. *Nature* **511**, 216–219 (2014).
7. Voogt, J. A. & Oke, T. R. Thermal remote sensing of urban climates. *Remote Sens. Environ.* **86**, 370–384 (2003).
8. Oke, T. R. Canyon geometry and the nocturnal urban heat island: comparison of scale model and field observations. *J. Climatol.* **1**, 237–254 (1981).
9. Taha, H. Urban climates and heat islands: albedo, evapotranspiration, and anthropogenic heat. *Energy Build* **25**, 99–103 (1997).
10. Mirzaei, P. A. & Haghighat, F. Approaches to study urban heat island—abilities and limitations. *Build. Environ.* **45**, 2192–2201 (2010).
11. Taha, H., Akbari, H., Sailor, D. & Ritschard, R. Causes and effects of heat islands: sensitivity to surface parameters and anthropogenic heating. *Lawrence Berkeley Lab. Rep.* 29864 (1992).
12. Imai, K. & Yamamoto, K. An evaluation of measures regarding road traffic against the urban heat island in the Tokyo Ward Area, Japan. *J. Environ. Prot. (Irvine, CA)* **6**, 957 (2015).
13. Louiza, H., Zéroual, A. & Djamel, H. Impact of the transport on the urban heat island. *Int. J. traffic Transp. Eng.* **5**, 252–263 (2015).
14. Kammuang-Lue, N., Sakulchangsatjatai, P., Sangnum, P. & Terdtoon, P. Influences of population, building, and traffic densities on urban heat island intensity in Chiang Mai City, Thailand. *Therm. Sci.* **15**, S445–S455 (2015).
15. Han, D., Yang, H. & Wang, X. Efficiency of the plate-number-based traffic rationing in general networks. *Transp. Res. Part E Logist. Transp. Rev.* **46**, 1095–1110 (2010).
16. US EPA, O. *Inventory of U.S. Greenhouse Gas Emissions and Sinks* (US EPA, 2018).
17. Zhong, S. & Yang, X. Q. Ensemble simulations of the urban effect on a summer rainfall event in the Great Beijing Metropolitan Area. *Atmos. Res.* **153**, 318–334 (2015).
18. Ren, G. Y., Chu, Z. Y., Chen, Z. H. & Ren, Y. Y. Implications of temporal change in urban heat island intensity observed at Beijing and Wuhan stations. *Geophys. Res. Lett.* **34**, (2007).
19. Li, R. & Guo, M. Effects of odd-even traffic restriction on travel speed and traffic volume: evidence from Beijing Olympic games. *J. Traffic Transp. Eng. (English Ed.)* **3**, 71–81 (2016).
20. Sun, Y., Zhang, X., Ren, G., Zwiers, F. W. & Hu, T. Contribution of urbanization to warming in China. *Nat. Clim. Chang.* **6**, 706–709 (2016).

21. Wang, F. Y., Tang, S., Sui, Y. & Wang, X. Toward intelligent transportation systems for the 2008 Olympics. *IEEE Intell. Syst.* **18**, 8–11 (2003).

22. Liu, M. J., Mao, B. H., Huang, Y., Zhang, J. P. & Chen, S. K. Comparison of pre- & post-Olympic traffic-a case study of several roads in Beijing. *Jiaotong Yunshu Xitong Gongcheng Yu Xinxi/ J. Transp. Syst. Eng. Inf. Technol.* **8**, 67–72 (2008).

23. Zhong, N., Cao, J. & Wang, Y. Traffic congestion, ambient air pollution, and health: evidence from driving restrictions in Beijing. *J. Assoc. Environ. Resour. Econ.* **4**, 821–856 (2017).

24. Shahmohamadi, P., Che-Ani, A. I., Maulud, K. N. A., Tawil, N. M. & Abdullah, N. A. G. The impact of anthropogenic heat on formation of urban heat island and energy consumption balance. *Urban Stud. Res.* **2011**, 1–9 (2011).

25. Meehl, G. A., Dropbox & Claudia. More intense, more frequent, and longer lasting heat waves in the 21st century. *Science* **305**, 994–997 (2004).

26. Zhou, Y. et al. The impact of transportation control measures on emission reductions during the 2008 Olympic Games in Beijing, China. *Atmos. Environ.* **44**, 285–293 (2010).

27. Cai, H. & Xie, S. Traffic-related air pollution modeling during the 2008 Beijing Olympic Games: the effects of an odd–even day traffic restriction scheme. *Sci. Total Environ.* **409**, 1935–1948 (2011).

28. Flanner, M. G. Integrating anthropogenic heat flux with global climate models. *Geophys. Res. Lett.* **36**, 1–5 (2009).

29. Li, Y. Y., Zhang, H. & Kainz, W. Monitoring patterns of urban heat islands of the fast-growing Shanghai metropolis, China: Using time-series of Landsat TM/ETM+ data. *Int. J. Appl. Earth Obs. Geoinf.* **19**, 127–138 (2012).

30. Liu, D. et al. Electricity consumption and economic growth nexus in Beijing: a causal analysis of quarterly sectoral data. *Renew. Sustain. Energy Rev.* **82**, 2498–2503 (2018).

31. National Bureau of Statistics, C. *Beijing Monthly/Anually Statistical Books.* https://data.stats.gov.cn/easyquery.htm?cn=E0101 (National Bureau of Statistics, 2008).

32. Li, Y. et al. Temporal variations of local traffic CO_2 emissions and its relationship with CO_2 flux in Beijing. *China. Transp. Res. Part D Transp. Environ.* **67**, 1–15 (2019).

33. Su, Y. et al. Transportation demand management for beijing 2008 Olympic games. In *2009 12th International IEEE Conference on Intelligent Transportation Systems* 1–6 (IEEE, 2009).

34. Road space rationing. *Wikipedia* https://en.wikipedia.org/wiki/Road_space_rationing.

35. Wang, S. et al. Quantifying the air pollutants emission reduction during the 2008 Olympic games in Beijing. *Environ. Sci. Technol.* **44**, 2490–2496 (2010).

36. Weng, Q., Lu, D. & Schubring, J. Estimation of land surface temperature-vegetation abundance relationship for urban heat island studies. *Remote Sens. Environ.* **89**, 467–483 (2004).

37. Oke, T. R., Spronken-Smith, R. A., Jáuregui, E. & Grimmond, C. S. B. The energy balance of central Mexico City during the dry season. *Atmos. Environ.* **33**, 3919–3930 (1999).

38. Georgescu, M., Morefield, P. E., Bierwagen, B. G. & Weaver, C. P. Urban adaptation can roll back warming of emerging megapolitan regions. *Proc. Natl. Acad. Sci. USA* **111**, 2909–2914 (2014).

39. Chen, H., Zhou, X., Dai, F. & Guan, Y. G. The study of urban ventilation corridor planning based on the accommodation of urban heat island and pollutions. *Mod. Urban Res.* **7**, 24–30 (2014).

40. Al Sakka, M., Gualous, H., Van Mierlo, J. & Culcu, H. Thermal modeling and heat management of supercapacitor modules for vehicle applications. *J. Power Sources* **194**, 581–587 (2009).

41. Jia, Y. et al. Estimated reduction in cancer risk due to PAH exposures if source control measures during the 2008 Beijing Olympics were sustained. *Environ. Health Perspect.* **119**, 815–820 (2011).

42. Ye, X. The effects of hot and cold temperatures on emergency hospital admissions in Brisbane, Australia (Doctoral dissertation, Queensland University of Technology, 2013).

43. Zhang, K., Thapa, B., Ross, M. & Gann, D. Remote sensing of seasonal changes and disturbances in mangrove forest: a case study from South Florida. *Ecosphere* **7**, 1–23 (2016).

44. Akbari, H., Pomerantz, M. & Taha, H. Cool surfaces and shade trees to reduce energy use and improve air quality in urban areas. *Sol. Energy* **70**, 295–310 (2001).

45. Mutiibwa, D., Strachan, S. & Albright, T. Land surface temperature and surface air temperature in complex terrain. *IEEE J. Sel. Top. Appl. Earth Obs. Remote Sens.* **8**, 4762–4774 (2015).

46. Norman, J. M., Kustas, W. P., Prueger, J. H. & Diak, G. R. Surface flux estimation using radiometric temperature: a dual temperature-difference method to minimize measurement errors. *Water Resour. Res.* **36**, 2263–2274 (2000).

47. Kato, S. & Yamaguchi, Y. Analysis of urban heat-island effect using ASTER and ETM+ data: separation of anthropogenic heat discharge and natural heat radiation from sensible heat flux. *Remote Sens. Environ.* **99**, 44–54 (2005).

48. Hardy, M. A. *Regression with Dummy Variables*, vol. 93 (Sage, 1993).

49. Liang, S. Narrowband to broadband conversions of land surface albedo I: Algorithms. *Remote Sens. Environ.* **76**, 213–238 (2001).

Author contributions

Competing interests

The authors declare no competing interests.

Additional information